

Fluctuation and Noise Letters  
 (2025) 2550003 (27 pages)  
 © World Scientific Publishing Company  
 DOI: 10.1142/S0219477525500038



## Reducing Random Valued Impulse Noise in Digital Color Images Using Clustering and Median Filtering

Srinivasa Rao Gantepalli

*Department of Electronics and Communication Engineering,  
 RGUKT ONGOLE, Ongole, India  
 srenivasaraog@rguktong.ac.in*

Praveen Babu Choppala \*

*Department of Electronics and Communication Engineering,  
 Andhra University, Visakhapatnam, India  
 praveenchoppala@andhrauniversity.edu.in*

Received 29 April 2024

Revised 26 July 2024

Accepted 28 July 2024

Published

Communicated by Stefania Residori

This paper proposes a new approach for filtering out impulse noise in digital color images. This work is of critical interest in biomedical imaging, visual tracking, etc. The conventional filtering methods operate by applying a noise reduction scheme, generally the vector median filtering approach and its variants, for the center pixel of a suitably chosen window that iteratively slides along the entire image. These methods consider the window in its entirety in the filtering process. This consideration, however, comprehends the noise within the noisy pixels in the filtering process and could prove detrimental to the overall output. The method proposed in this paper operates by clustering the pixels in the chosen window into two groups, one that corresponds to the pixel intensities that lie in the signal space and the other to those that lie in the noise space. The motivating rationale for this clustering scheme is to marginalize those pixels that lie in the noise space that seemingly do not contribute to the information in the image. The median filter is then applied to the pixels that contribute to the signal, in isolation from the color components, to filter out the impulse noise. Simulation results show that the proposed method outperforms conventional filtering methods in terms of noise reduction and structural similarity and thus validates the proposed approach. The proposed method is applied to analyze CT scans for improved diagnosis of SARS-COV-2 COVID-19 disease. The method is also applied to a visual tracking example as a preprocessor.

*Keywords:* Impulse noise; vector median filters; directional filters;  $k$ -means clustering; isolated median filtering; root mean square error.

\*Corresponding author.

*S. R. Gantengapalli & P. B. Choppala*

## 1. Introduction

Digital color imaging, which involves capturing and representing real-world scenes in terms of RGB (red, green, blue) pixel intensities, is prone to noise such as impulse noise and salt-and-pepper noise. These unwanted artifacts can significantly degrade image quality, leading to loss of important details and flawed interpretation, especially in critical applications like biomedical imaging, visual tracking and electron tomography [1].

Impulse noise typically appears as randomly occurring white and black pixels, caused by sudden disturbances during the image acquisition process or transmission errors. This noise not only diminishes the visual quality of the image but also poses significant challenges for image processing algorithms that rely on clear and accurate image data. Effective noise reduction is crucial to ensure the accuracy and reliability of images in these applications. Several techniques have been developed to address this issue. Traditional methods like median filtering are widely used due to their simplicity and effectiveness in removing salt-and-pepper noise while preserving edges. Median filtering replaces each pixel's value with the median value of its neighboring pixels, thus effectively reducing noise without significantly blurring the image. From this standpoint, the basis of this paper is to develop novel methods for reducing noise in digital color images that will be applicable to all classes for image processing applications.

Developing effective noise reduction techniques for digital color images is essential for ensuring high-quality, reliable images in various applications. Ongoing research continues to explore and improve these methods, incorporating advances in adaptive filtering, wavelet transforms and deep learning to tackle the challenges posed by noise in digital imaging. Several approaches have been proposed over the years to filter out impulse noise in color images albeit most research is limited to grayscale images.

The median filtering approaches are by far the most popular image filtering ones due to their robustness to noise. The general idea of these methods is to examine and correct a test pixel's (usually the center pixel) representativeness of a selected window (a set of surrounding pixels) within the image. The simplest noise reduction filter in this category is the standard median filter that computes the pixel median for each selected window over each color component and replaces the test pixel with the median [2–4].

The vector median filter (VMF) is a prominently used order-reducing scheme that processes color images as a vector field [5, 6]. This method works by replacing the test pixel with another pixel in the window that minimizes the aggregate distance across all pixels. An alternative to using distance is the use of direction as proposed in the basic vector directional filter (BVDF) [7]. This filter rather uses the angular distance between the pixels than the vector magnitudes and minimizes the aggregate angular distance across all pixels in the window. Another approach to image filtering includes directional distance filtering (DDF) which utilizes a weighted product of VMF and BVDF [8].

*Reducing Random-Valued Impulse Noise in Digital Color Images*

The directional VMF (DVMF) is another directional scheme that operates by performing vector median filtering across the pixels that lie within, degrees from the center test pixel and then taking the VMF for the resultant [9]. The filters of this family, and especially the VMF and directional filters can perform quite robustly especially when the correlation between the three-color components has to be preserved [10]. The problem however in these methods is that the vector pixel is processed jointly as a multichannel. Consequently, any smoothing performed therein is accounted for in all the color channels equally. This could be problematic because outliers in one color component may influence the others thereby corrupting some good pixels.

Recent work in reducing impulsive noise in digital color images can be largely attributed to the work of Smolka *et al.* Their contributions include the adaptive rank-weighted switching filter (ARWSF) [12] and the adaptive switching trimmed (AST) filters and others. These methods have shown promise and superiority in reducing impulsive noise. Other techniques for noise reduction include extended versions of VMF like the alpha trimmed VMF [11], adaptive switching filters [12], peer-group filters [13] and the adaptive weighted directional difference methods [14]. We neglect these as they are either limited to grayscale images or perform comparably to the aforementioned techniques or are not specific to filtering based on a directional approach. Moreover, research into noise reduction in images is twofold: (a) detecting whether a pixel is corrupted by impulse noise which is relatively difficult in random valued impulse noise and (b) filtering out the noise [15]. The focus of this paper is only on the latter.

This paper proposes a new filtering approach to reduce impulse noise in digital color images. This method operates by clustering the pixels in a chosen sliding window into two groups, the first that encompasses the signal and the second that encompasses the noise. Use the well-known  $k$ -means method with  $K = 2$  to accomplish this clustering based on the pixel intensities [19]. The key rationale in grouping the pixels in a sliding window into signal and noise components is that the pixels that encompass the signal will be numerous and will have their intensities in close proximity while those that encompass the noise will be few and will have their intensities distant from those corresponding to the signal space. Based on the said rationale, the cluster having the maximum number of pixels will encompass the signal space. The pixels in this cluster are filtered using the median filter to determine the new value of the test (center) pixel. The median filter is applied on isolated color components to avoid the effect of the filtering process being leveraged in the adjacent color components. This method, in essence, uses those pixels that seemingly contribute to the signal, and thereby we mitigate the effect of the corrupted pixels in the filtering process. This approach will result in improved accuracy. Our simulation results show that the proposed method outperforms the state-of-the-art impulse noise reduction filters.

Our simulation results show that the proposed method outperforms the state-of-the-art impulse noise reduction filters. The proposed method is straightforwardly

*S. R. Gantepalli & P. B. Choppala*

applicable to grayscale images also and is applied to chest computed tomography (CT) scan images of COVID-19 patients and its efficacy for improved diagnosis is discussed. The proposal is also applied as a preprocessing tool for visual tracking examples with condensing results.

The rest of the paper is organized as follows. Section 2 sets the notation and describes the impulse noise. This is followed by the conventional impulse noise reduction methods in Sec. 3 and the proposed Isolated Vector Median Filtering using  $k$ -means clustering (IMF-KM) filter in Sec. 4. Then we present the results in Sec. 5 and conclude in Sec. 6.

## 2. The Impulse Noise Model

In this section, we set the notation and describe the impulse noise model for a digital color image. Let  $\mathbf{X}$  be the color image of  $M \times N$  pixels containing  $MN$  pixels where  $M$  denotes the number of rows and  $N$  the number of columns. Then the color image  $\mathbf{X}$  will be a set of vector pixels

$$\mathbf{X} = \{\mathbf{x}_{i,j}, i = 1, 2, \dots, M, j = 1, 2, \dots, N\}, \quad (1)$$

with each pixel being a joint vector containing the color intensities in the red, green and blue components as

$$\mathbf{x}_{i,j} = (x_{i,j,r}, x_{i,j,g}, x_{i,j,b}), \quad i = 1, \dots, M, \quad j = 1, \dots, N. \quad (2)$$

Let  $\mathbf{Z} = (\mathbf{z}_{i,j}, i = 1, \dots, M, j = 1, \dots, N)$  be the image corrupted by impulse noise. As discussed earlier, impulse noise is mainly classified as fixed-valued impulse noise (a.k.a. salt-and-pepper noise) and random-valued impulse noise. In the fixed-valued impulse noise, a pixel is corrupted with probability  $p \in (0,1)$ . A corrupted pixel implies that one of its red, green or blue components gets corrupted by a railing to 0 (full black) or 255 (full white) with uniform probability across the color components. In the random valued impulse noise, the corrupted pixels take any random value between 0 and 255 instead of railing to high or low values. This model, in general, can be described as

$$\mathbf{z}_{i,j} = \begin{cases} \mathbf{x}_{i,j} & \text{if } q \geq p, \\ (x_{i,j,r}, x_{i,j,g}, a) & \text{if } q < p \leq r < \frac{2}{3}, \\ (x_{i,j,r}, a, x_{i,j,b}) & \text{if } q < p, \quad \frac{1}{3} \leq r < \frac{2}{3}, \\ (a, x_{i,j,g}, x_{i,j,b}) & \text{if } q < p, \quad \frac{2}{3} \leq r, \end{cases} \quad (3)$$

where  $(r, q) \in (0,1)$  are continuous random numbers chosen uniformly and  $a = 0$  or 255 is uniformly chosen for fixed valued impulse noise,  $a \in (0, 255)$  is uniformly chosen within the interval for random valued impulse noise. This description indicates that  $p$  denotes the noise probability of an image and the closer the value of  $p$  to one, the

## Reducing Random-Valued Impulse Noise in Digital Color Images

higher the noise and the closer the value of  $p$  to zero, the lower the noise. The aim of noise reduction techniques is to restore the original image from the noisy image.

### 3. Conventional Noise Reduction Filters

In this section, we describe the conventional impulse noise filtering methods in brief. The filtering process in general uses a sliding window  $W$  containing  $n$  pixels and of size  $\sqrt{n} \times \sqrt{n}$ . For convenience, we denote the set of pixels contained in the window as

$$W = \{\mathbf{x}_i, i = 1, \dots, n\}, \quad (4)$$

where the joint vector is  $\mathbf{x}_i = \{x_{i,r}, x_{i,g}, x_{i,b}\}$ . With this notation, the digital color image in Eq. (1) is now modified as

$$\mathbf{X} = \{\mathbf{x}_i, i = 1, \dots, MN\}. \quad (5)$$

The filtering methods operate by detecting and processing the center pixel within the test window  $W$ . An example of the test window is shown in Fig. 1. The most prominent of all filtering schemes are the VMF method. Here the aggregated distance of each pixel from every other pixel is computed as

$$S_i = \sum_{j=1}^n d(\mathbf{x}_i - \mathbf{x}_j), \quad i = 1, 2, \dots, n, \quad (6)$$

where  $d(\mathbf{x}_i - \mathbf{x}_j)$  is Minowski's distance between two joint pixels  $\mathbf{x}_i$  and  $\mathbf{x}_j$ , and reorder the aggregate as

$$S_{\hat{i}=1, \dots, n} \Rightarrow \mathbf{x}_{\hat{i}=1, \dots, n} : S_{\hat{i}=1} \leq S_{\hat{i}=2} \leq \dots \leq S_{\hat{i}=n}. \quad (7)$$

Then the center pixel is replaced with the pixel having the minimum aggregate distance from all other pixels as

$$\mathbf{x}_c = \mathbf{x}_{\hat{i}-1}. \quad (8)$$

The BVDF, on the contrary, uses the aggregate angular distance between the pixels as

$$\theta_i = \sum_{j=1}^n \cos^{-1} \left( \frac{\mathbf{x}_i \cdot \mathbf{x}_j}{\|\mathbf{x}_i\| \|\mathbf{x}_j\|} \right), \quad i = 1, 2, \dots, n, \quad (9)$$

$\mathbf{x}_1$	$\mathbf{x}_4$	$\mathbf{x}_7$
$\mathbf{x}_2$	$\mathbf{x}_c = \mathbf{x}_5$	$\mathbf{x}_8$
$\mathbf{x}_3$	$\mathbf{x}_6$	$\mathbf{x}_9$

Fig. 1. An example  $3 \times 3$  test window with  $n = 3^2 = 9$ . The center pixel is the test pixel.

*S. R. Gantengapalli & P. B. Choppala*

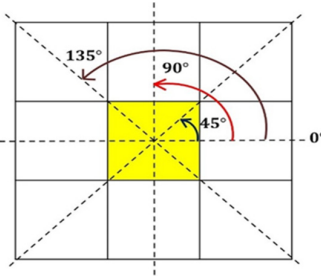


Fig. 2. A pictorial representation of DVMF.

and replaces the center pixel with the pixel that minimizes as described in Eqs. (7) and (8). The DDF uses the weighted product of Minkowski's distance and the angular distance as

$$\mathbf{A}_i = \mathbf{G}_i^\gamma \theta_i^{(1-\gamma)}, \quad i = 1, 2, \dots, n, \quad (10)$$

where  $\gamma \in (0, 1)$ . The DVMF filter operates by taking the VMF of the pixels lying in degrees to the center pixel as shown in Fig. 2 and then taking the VMF of the resultant. The VMFDD approach takes the sum of the distances along with four different directions and then selects those pixels that lie in the angle that minimizes the sum from the center pixel and VMF is performed over those pixels. The alpha-trimming approach trims the distances by a chosen trimming factor  $\alpha$  while the AST method applies a switching condition for the trimming process.

In all these methods, the focus is on reducing the noise by applying the VMF mechanism in different variants. There is little work in identifying pixels that correspond to noise and mitigating their effect in the filtering process. The peer group filter attempted this approach but was limited to grayscale images. The recently proposed ARWSF ranks combine the process of identifying good pixels (those that contribute to the signal/information) by first computing the distances of the pixels  $d(\cdot)$  in the sliding window and then scaling the distances using a decaying function. This scaling gives high weighting to those pixels having minimum aggregate distance. Performing VMF over pixels using the scaling results in improved noise reduction as the most informative pixels are weighted highly in the filtering process. In the subsequent section, we propose the IMF-KM method which improves the ARWSF method and fully marginalizes the noise pixels for improved noise reduction.

#### 4. Proposed Method

The clustering process in the proposed method involves segmenting an image into regions based on two distinct values. Initially, the image is processed to extract the feature vectors representing these two values, which could be color intensities, texture patterns or any other relevant metrics. These feature vectors are then analyzed

### Reducing Random-Valued Impulse Noise in Digital Color Images

to identify natural groupings or clusters. A clustering algorithm, such as  $k$ -means or hierarchical clustering, is employed to partition the data into clusters based on similarity. The algorithm iterates to refine the cluster boundaries, minimizing the intra-cluster variance and maximizing the inter-cluster variance. Once the clusters are established, each pixel in the image is assigned to the nearest cluster, effectively segmenting the image into regions with homogeneous properties corresponding to the two values. This process helps in highlighting the structural differences in the image based on the chosen values, facilitating further analysis or interpretation.

#### **4.1. Motivation**

The key idea of the proposed IMF-KM method is two-fold: (a) to categorize the pixels in the sliding window into two groups, one that contributes to the signal and the other that contributes to the noise and (b) to perform median filtering, in isolation of the color components, over the pixel intensities that contribute to the signal. Step (a) categorizes the pixels based on the spatial placement of their intensities using the  $k$ -means clustering algorithm [16]. The cluster of intensities that contribute to the signal is then processed via the median filter. This process is performed in isolation over the color components to avoid the effect of smoothing or softening or smearing in one color component leveraging itself on the rest. We chose this approach as it was found to be effective in reducing impulsive noise in several images [17, 18].

#### **4.2. Proposed methodology**

Consider a sliding window  $W = \{\mathbf{x}_i, i = 1, \dots, n\}$  containing  $n$  pixels. From  $W$ , we obtain the isolated color sliding windows as

$$W_r = \{x_{r,i}, i = 1, \dots, n\}, \quad (11)$$

$$W_g = \{x_{g,i}, i = 1, \dots, n\}, \quad (12)$$

$$W_b = \{x_{b,i}, i = 1, \dots, n\}. \quad (13)$$

The reader is notified that the methodology proposed in the sequel corresponds to the red color component and should be extended to the green and blue components as is in isolation of the color components. Consider the sliding window corresponding to the red component  $W_r = \{x_{r,i}, i = 1, \dots, n\}$ . This window contains the red component pixel intensities. These intensity values are then clustered into two groups using the unsupervised learning method, the  $k$ -means method [19] with  $K = 2$ . The  $k$ -means method over the sliding window results in a responsibility vector

$$\mathbf{R}_r = \{j_i, j_i \in (1, 2), i = 1, \dots, n\}, \quad (14)$$

$$\mathbf{R}_r = \{j_{i=1,\dots,n} = 1\} \cup \{j_{i=1,\dots,n} = 2\}, \quad (15)$$

$$\mathbf{R}_r = \mathbf{R}_r[1] \cup \mathbf{R}_r[2], \quad (16)$$

*S. R. Gantengapalli & P. B. Choppala*

such that the  $i$ th responsibility variable  $j_i$  takes any of the two values, 1 or 2, indicating the cluster number to which the  $i$ th pixel intensity  $x_{r,i}$  belongs. The set  $\mathbf{R}_r[1]$  contains the indices. This lets us categorize the  $n$  pixels into two clusters as

$$\mathbf{C}_r[1] = \{x_{j_i,r} : j_i = 1\}, \quad i = 1, \dots, n, \quad (17)$$

$$\mathbf{C}_r[2] = \{x_{j_i,r} : j_i = 2\}, \quad i = 1, \dots, n. \quad (18)$$

We then take the cluster containing the maximum pixel values according to

$$\eta_r = \mathbf{C}_r[j] \text{s.t.} |\mathbf{C}_r[j]| > |\mathbf{C}_r[i \in (1, 2), i \neq j]|, \quad (19)$$

where  $|\cdot|$  of a set denotes its cardinality. Essentially, this method clusters the pixel intensities in the sliding window into two groups, the first — the dominant set  $\eta_r$  assumingly lying in the signal space, and the second assumingly lying in the noise space. We assume since the dominant set has more pixel intensities spaced close to one another, they contribute to the signal part of the image and the other set contributes to the noise. We can then perform median filtering over the pixel intensities in the dominant set and replace the red component of the center test pixel as

$$x_{c,r} = \text{Median}(\eta_r). \quad (20)$$

The process is repeated over green and blue color components in isolation and we obtain the final test pixel as

$$\mathbf{x}_c = (x_{c,r}, x_{c,g}, x_{c,b}). \quad (21)$$

The  $k$ -means algorithm employed to cluster the pixel intensities in the red color component and to obtain the responsibility vector  $\hat{\mathbf{R}}_r$  in Eq. (4) is outlined in Algorithm 1. The proposed IMF-KM method for the red color component is outlined in Algorithm 2.

---

**Algorithm 1.** The  $k$ -means algorithm.

---

**$R_r = K\text{-MEANS } [\{x_{i,r}, i = 1, \dots, n\}, K]$**

    Initialize centroids  $c_k = 1, \dots, K$  at random.

**while** Flag Up **do**

        Compute distance  $\mathbf{D}(i, k) = d(x_{i,r} - c_k), i = 1, \dots, n, k = 1, \dots, K$

        where  $d(\cdot)$  is any distance measure.

        Compute responsibility vector

$\mathbf{R}_r = \{j_i = k : \text{argmin}_k \mathbf{D}(i, k), i = 1, \dots, n\}$ . That is, the  $i$ th sample will belong to the  $j_i$ th cluster that minimizes its distance over the centroids.

        Compute new centroids

$c_k = \sum x_{j_i=k,r} / |\{j_i = k, i = 1, \dots, n\}|, k = 1, \dots, K$

**if**  $c_k, k = 1, \dots, K$  values unchanged **then** Flag Down

**end if**

**end while**

---

## Reducing Random-Valued Impulse Noise in Digital Color Images

---

**Algorithm 2.** The proposed **IMF-KM** algorithm.

---

$$x_{c,r} = \text{IMF-KM}[W_r = \{x_{i,r}, i = 1, \dots, n\}]$$

Cluster the pixel intensities using  $k$ -means algorithm and obtain responsibility vector  $\mathbf{R}_r = \mathbf{K}\text{-MEANS } [\{x_{i,r}, i = 1, \dots, n\}, K = 2]$

Categorise the  $n$  pixels into two clusters

$$C_r[j] = \{x_{j_{i,r}} : j_i = 1\}, i = 1, \dots, n, j = 1, 2$$

Determine the dominant cluster  $\eta_r$  according to Eq. (9).

The center test pixel is  $x_{c,r} = \text{Median}(\eta_r)$

---

## 5. Simulation and Comparison

In this section, we compare the proposed IMF-KM with state-of-the-art vector median filters using three test statistics.

The first is the root mean square error (RMSE) defined as

$$\text{RMSE}(\mathbf{X}, \mathbf{Y}) = \sqrt{\frac{1}{MN} \sum_{i=1}^M \sum_{j=1}^N \|\mathbf{X}_{i,j} - \mathbf{Y}_{i,j}\|^2}, \quad (22)$$

where  $\mathbf{X}$ ,  $\mathbf{Y}$ , respectively, are the original and filtered images. A small RMSE value indicates that the error between the filtered image and the original is minimal, reflecting high accuracy in image restoration. This low error signifies that the filtering process effectively preserves the original image's details while reducing noise. Consequently, achieving small RMSE values is desirable, as it demonstrates the method's efficiency in maintaining image quality. The closer the RMSE value is to zero, the better the filtered image matches the original. Thus, low RMSE values are a key objective in image filtering and restoration processes. The second measure is the peak signal-to-noise ratio (PSNR) defined as

$$\text{PSNR}(\mathbf{X}, \mathbf{Y}) = 10 \log_{10} \left( \frac{\text{Max}(\mathbf{X})^2}{\text{MSE}(\mathbf{X}, \mathbf{Y})} \right), \quad (23)$$

where  $\text{MSE}(\mathbf{X}, \mathbf{Y})$  is the mean square error of the filtered image. A high PSNR value indicates that the filtered image is very similar to the original image, demonstrating effective noise reduction and preservation of image quality. The Peak Signal-to-Noise Ratio (PSNR) measures the ratio between the maximum possible power of a signal and the power of corrupting noise, with higher values representing better image restoration. A high PSNR value suggests that the filtering process has successfully minimized distortion and artifacts. Consequently, achieving high PSNR values is desirable, as it reflects the method's ability to produce a high-quality, clear image. The third measure is the structural similarity index (SSIM) defined as

$$\text{SSIM}(\mathbf{X}, \mathbf{Y}) = \frac{(2\mu_x\mu_y + c_1)(2\sigma_{X,Y} + c_2)}{(\mu_x^2 + \mu_y^2 + c_1)(\sigma_x^2 + \sigma_y^2 + c_2)}, \quad (24)$$

*S. R. Gantepalli & P. B. Choppala*

where the image means are

$$\mu_x = \frac{1}{N} \sum_{i=1}^M \sum_{j=1}^N \mathbf{X}_{i,j}, \quad (25)$$

$$\mu_y = \frac{1}{N} \sum_{i=1}^M \sum_{j=1}^N \mathbf{Y}_{i,j}, \quad (26)$$

and  $\sigma_2(\cdot)$  denotes the variance and  $C(\cdot, \cdot)$  denotes the covariance between the original and filtered images. The SSIM value denotes the similarity between two images, the original and the filtered in our case, by incorporating perceptual features including luminance and contrast. A high value of SSIM indicates an accurate reconstruction of the original image. An overview of these comparative measures can be found in Ref. 12.

We first demonstrate the superiority of the proposed IMF-KM method over state-of-the-art filtering methods. In Fig. 3, we display the test case image used for this purpose. For this test case, Fig. 4 shows the noisy image and the filtered images at varying noise probabilities and it can be visually observed that the last column corresponding to the proposed IMF-KM method outperforms the other methods.

For the demonstration in Fig. 4, the RMSE, the PSNR and the SSIM performance versus the noise probability are shown in Figs. 5(a)–5(c), respectively. It can be seen that our IMF-KM method shows improved accuracy (i.e., low RMSE) than that of the joint vector approaches and also the IVMDF approach and the efficiency will increase with the increase in noise probability.

In terms of the RMSE, the method exhibits only 0.7 times the efficiency of the VMF at  $p = 0.2$ . However, its performance improves from  $p = 0.4$  and is twice better at  $p = 0.6$  and nearly 2.34 times better at  $p = 0.95$ . This tremendous improvement



Fig. 3. The original test image.

## Reducing Random-Valued Impulse Noise in Digital Color Images



Fig. 4. Left to right: (a) Noisy image, (b) Median filter, (c) VMF, (d) BVDF, (e) DDF, (f) DVMF, (g) VMFDD, (h) ARWSF, (i)  $\alpha$  trim, (j) AST, (k) IMF-KM. Top to bottom: noise probability  $p = 0.1, 0.2, 0.3, 0.4, 0.5, 0.6, 0.7, 0.8, 0.9, 0.95$ .

could be attributed to the best use of pixels that contribute to the information in the sliding window. The superiority can also be explained in terms of structural similarity. The proposed IMF-KM method shows only a 0.7% improvement over the VMF method at  $p = 0.2$  but this becomes increasingly efficient to about 15% at  $p = 0.95$ . This shows that the isolated median filtering of only the useful pixels, i.e., those pixels that lie in the signal space and supposedly contain useful information, will result in improved impulse noise reduction. This assertion is validated by testing over another four images to prove the robustness of the proposal.

In Figs. 6–8, we show the original test case images. For these test cases, Fig. 9–11 correspondingly show the noisy image and the filtered images at varying noise probabilities and it can be visually observed that the last column corresponding to

*S. R. Gantengapalli & P. B. Choppala*

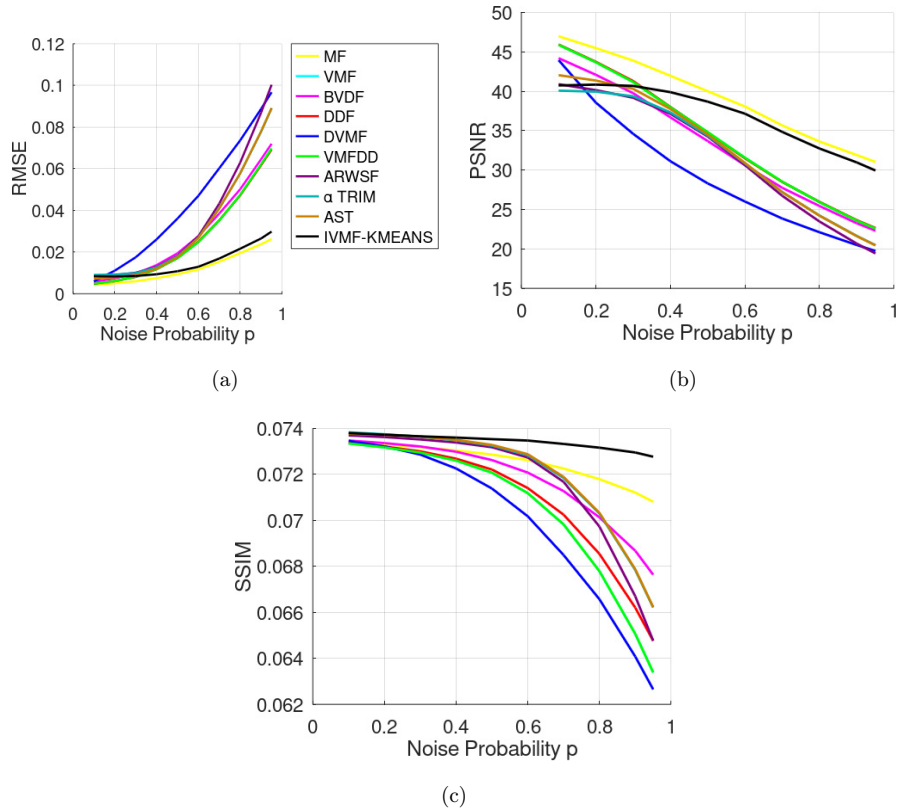


Fig. 5. (a) The RMSE versus the noise probability, (b) the PSNR versus the noise probability and (c) the SSIM versus the noise probability.



Fig. 6. The original test image.

*Reducing Random-Valued Impulse Noise in Digital Color Images*

Fig. 7. The original test image.

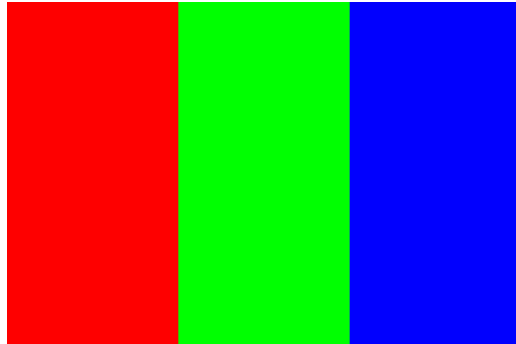


Fig. 8. The original test image.

the proposed IMF-KM method outperforms the other methods. The corresponding RMSE, PSNR and SSIM values are shown in Fig. 12. From all the five test cases, it can be observed that the proposed IMF-KM method outperforms all other methods and shows similar performance across all test cases and across all values of  $p$ .

The RMSE, PSNR and SSIM performance statistics indicate that of all the tested methods the VMF and the DVMF methods compare favorably to the proposed IMF-KM method despite the latter showing tremendous superiority of the former. Table 1 shows the ratio of the RMSE of the VMF and the DVMF methods to the proposed IMF-KM method for  $p$  from 0.5 to 0.95. Since we desire low RMSE values, the expected ratio should be greater than one. It can be observed that indeed for all the four test images, the ratio is more than 1.5 indicating a 50% improvement by the proposed method. Tables 2 and 3 show the ratio of the PSNR and SSIM values

*S. R. Gantengapalli & P. B. Choppala*

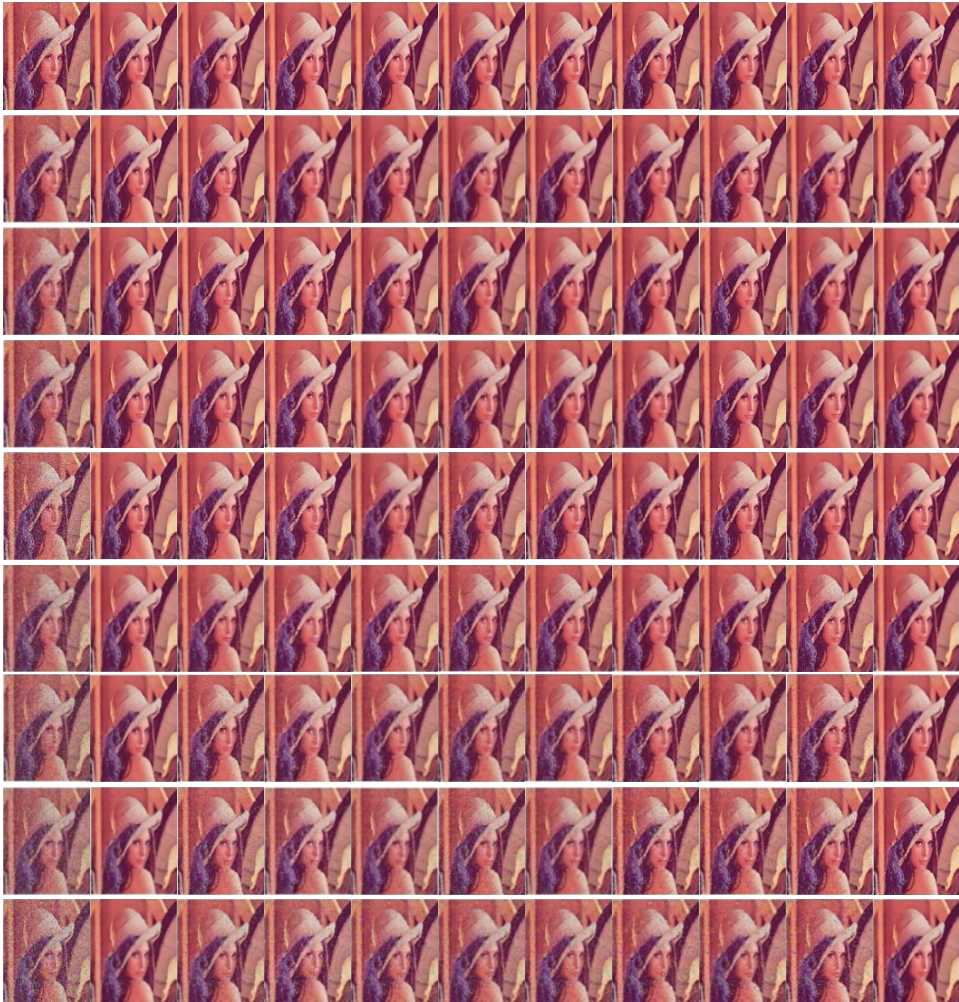


Fig. 9. Left to right: (a) noisy image, (b) median filter, (c) VMF, (d) BVDF, (e) DDF, (f) DVMF, (g) VMFDD, (h) ARWSF, (i)  $\alpha$  trim, (j) AST and (k) IMF-KM. Top to bottom: noise probability  $p = 0.1, 0.2, 0.3, 0.4, 0.5, 0.6, 0.7, 0.8, 0.9, 0.95$ .

of the VMF and the DVMF methods compared to the proposed IMF-KM method for  $p$  values ranging from 0.5 to 0.95. Since higher PSNR and SSIM values are desired, the expected ratio should be less than one. As shown in the tables, for all four test images, the ratio remains consistently less than one, indicating that the proposed IMF-KM method outperforms the VMF and DVMF methods across the tested  $p$  values.

These results, in summary, show that the proposed idea of clustering pixels within a test window to identify those that contain information and then filtering those pixels can result in an improved reduction of impulse noise in digital color images.

## Reducing Random-Valued Impulse Noise in Digital Color Images

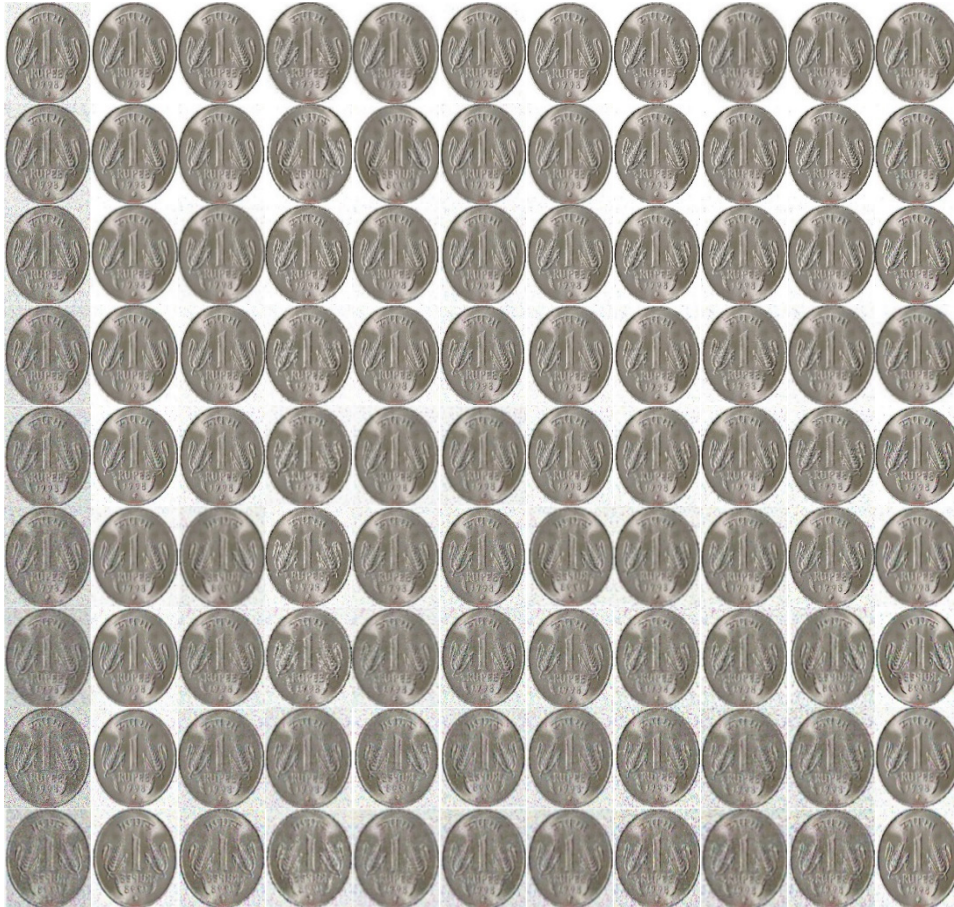


Fig. 10. Left to right: (a) noisy image, (b) Median filter, (c) VMF, (d) BVDF, (e) DDF, (f) DVMF, (g) VMFDD, (h) ARWSF, (i)  $\alpha$  trim, (j) AST and (k) IMF-KM. Top to bottom: Noise probability  $p = 0.1, 0.2, 0.3, 0.4, 0.5, 0.6, 0.7, 0.8, 0.9, 0.95$ .

Table 4 shows the average results from four test cases of RMSE value comparing the proposed method to conventional methods. The proposed method demonstrates an improvement of over 46% compared to the ARWSF method, 42% compared to the AST method and 33% compared to the VMF method, particularly at higher probability values.

Table 5 presents the average PSNR results from four test cases, comparing the proposed method with conventional methods. The proposed method achieves an improvement of over 26% compared to the ARWSF method, 22% compared to the AST method and 16% compared to the VMF method, especially at higher probability values. Table 6 gives over 15% compared to the ARWSF method 20% compared to the AST method, 20% compared to the VMF method.

*S. R. Gantepalli & P. B. Choppala*



Fig. 11. Left to right: (a) noisy image, (b) median filter, (c) VMF, (d) BVDF, (e) DDF, (f) DVMF, (g) VMFDD, (h) ARWSF, (i)  $\alpha$  trim, (j) AST and (k) IMF-KM. Top to bottom: Noise probability  $p = 0.1, 0.2, 0.3, 0.4, 0.5, 0.6, 0.7, 0.8, 0.9, 0.95$ .

### 5.1. Application to SARS-CoV2 (COVID-19) diagnosis

The severe acute respiratory syndrome SARS-CoV2 coronavirus disease (COVID-19) outbreak has shattered many lives, families and national economies with over 420 million reported cases and nearly 6 million deaths (courtesy: <https://www.worldometers.info/coronavirus>). The medical fraternity with all its sophisticated diagnosis and treatment facility has been seriously challenged globally in handling the outbreak. Research has shown that the chest CT scan is an important measure of

## Reducing Random-Valued Impulse Noise in Digital Color Images

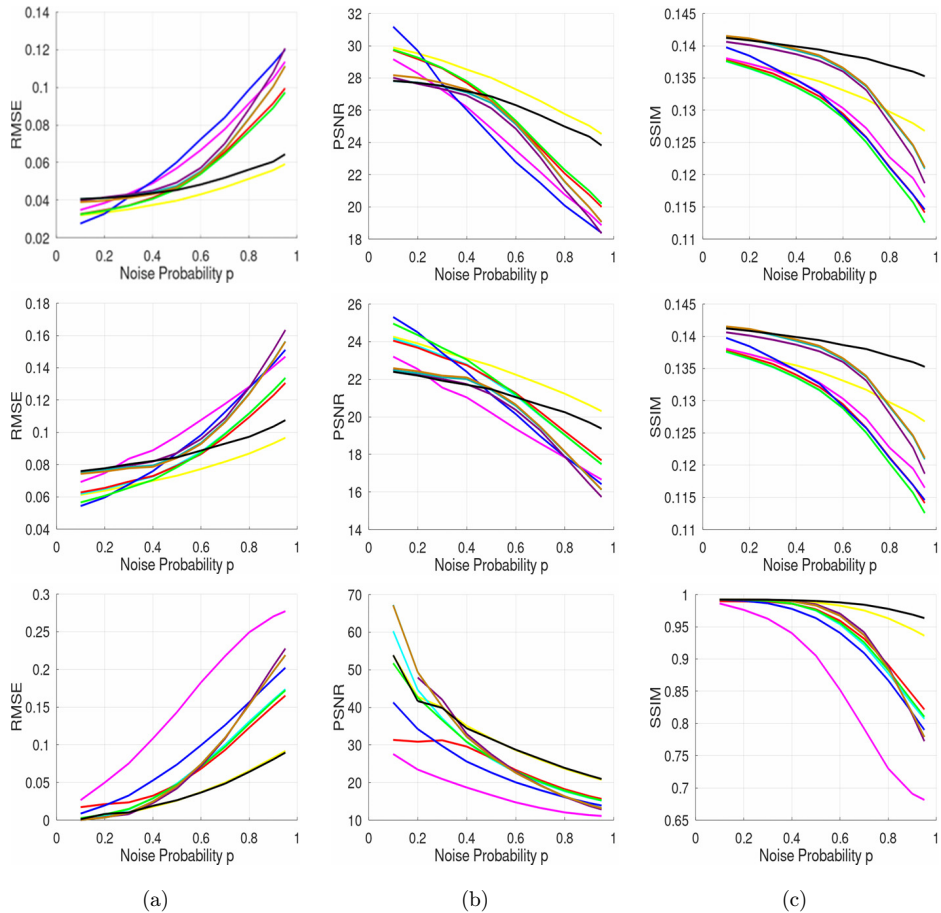


Fig. 12. The columns from Left to right correspond to (a) the RMSE versus the noise probability, (b) the PSNR versus the noise probability (c) the SSIM versus the noise probability. The rows from top to bottom correspond to the test images in Figs. 6–8, respectively. The legend of these figures is the same as shown in Fig. 5(a) and not shown here.

Table 1. The ratio of the RMSE of the VMF and DVMF methods to the IMF-KM method.

<i>P</i>	Test image 1		Test image 2		Test image 3		Test image 4	
<b>0.5</b>	1.5817	1.5882	1.0115	1.032	0.9438	0.9379	1.8422	1.783
<b>0.6</b>	1.9165	1.9346	1.1171	1.1392	0.9903	0.9752	2.0031	1.8638
<b>0.7</b>	2.0827	2.0897	1.2398	1.2607	1.0681	1.0442	2.0673	1.9223
<b>0.8</b>	2.1938	2.1866	1.3588	1.3931	1.1503	1.1256	2.0445	1.9179
<b>0.9</b>	2.3415	2.3283	1.4709	1.5109	1.2173	1.1866	1.9854	1.8807
<b>0.95</b>	2.3369	2.3203	1.5103	1.5442	1.2435	1.2146	1.938	1.8431

*S. R. Gantepalli & P. B. Choppala*

Table 2. The ratio of the PSNR of the VMF and DVMF methods to the IMF-KM method.

<b>P</b>	Test image 1		Test image 2		Test image 3		Test image 4	
<b>0.5</b>	0.8998	0.8989	0.9963	0.9897	1.0234	1.0259	0.8323	0.8407
<b>0.6</b>	0.8495	0.8475	0.9631	0.9566	1.0040	1.0103	0.7902	0.8119
<b>0.7</b>	0.8186	0.8178	0.9266	0.9208	0.9722	0.9818	0.7602	0.7842
<b>0.8</b>	0.7921	0.7931	0.8923	0.8834	0.9399	0.9493	0.7399	0.7632
<b>0.9</b>	0.7618	0.7634	0.8615	0.8516	0.9133	0.9246	0.7278	0.7493
<b>0.95</b>	0.7542	0.7563	0.8484	0.8399	0.9023	0.9128	0.7257	0.7465

Table 3. The ratio of the SSIM of the VMF and DVMF methods to the IMF-KM method.

<b>P</b>	Test image 1		Test image 2		Test image 3		Test image 4	
<b>0.5</b>	0.9801	0.982	0.9442	0.9478	0.9277	0.9337	0.9849	0.9869
<b>0.6</b>	0.9688	0.9719	0.9292	0.9338	0.9137	0.9228	0.9655	0.9712
<b>0.7</b>	0.9522	0.958	0.9057	0.9114	0.8829	0.8967	0.9368	0.9465
<b>0.8</b>	0.9266	0.9369	0.8782	0.8849	0.8500	0.8651	0.8976	0.9111
<b>0.9</b>	0.8919	0.9075	0.8508	0.8598	0.8215	0.8400	0.8564	0.8717
<b>0.95</b>	0.8711	0.8900	0.8322	0.8436	0.8039	0.8202	0.8378	0.8528

Table 4. The RMSE of the VMF, ARWSF and AST methods to the IMF-KM method.

<b>P</b>	VMF	ARWSF	AST	IMF-KM	VMF (%↓)	ARWSF (%↓)	AST (%↓)
<b>0.1</b>	0.03267	0.03952	0.03911	0.04030	-23.3642	-1.971	-3.027
<b>0.2</b>	0.03443	0.04125	0.04008	0.04109	-19.344	0.385	-2.510
<b>0.3</b>	0.03654	0.04259	0.04102	0.04219	-15.451	0.942	-2.852
<b>0.4</b>	0.04052	0.04530	0.04327	0.04371	-7.877	3.505	-1.028
<b>0.5</b>	0.04614	0.04962	0.04725	0.04575	0.845	7.798	3.175
<b>0.6</b>	0.05359	0.05806	0.05498	0.04757	11.229	18.062	13.473
<b>0.7</b>	0.06335	0.06951	0.06665	0.05184	18.167	25.426	22.229
<b>0.8</b>	0.07582	0.08860	0.08357	0.05612	25.983	36.653	32.846
<b>0.9</b>	0.09017	0.10952	0.10169	0.06065	32.736	44.616	40.356
<b>0.95</b>	0.09942	0.12465	0.11495	0.06613	<b>33.485</b>	<b>46.946</b>	<b>42.471</b>

Table 5. The RMSE of the VMF, ARWSF and AST methods to the IMF-KM method.

<b>P</b>	VMF	ARWSF	AST	IMF-KM	VMF (%↑)	ARWSF (%↑)	AST (%↑)
<b>0.1</b>	29.718	28.063	28.151	27.893	-6.141	-0.606	-0.916
<b>0.2</b>	29.261	27.69	27.939	27.724	-5.253	0.123	-0.770
<b>0.3</b>	28.744	27.412	27.739	27.494	-4.349	0.299	-0.883
<b>0.4</b>	27.846	26.876	27.275	27.185	-2.374	1.150	-0.330
<b>0.5</b>	26.715	26.084	26.509	26.79	0.281	2.707	1.060
<b>0.6</b>	25.409	24.718	25.19	26.449	4.093	7.003	4.998
<b>0.7</b>	23.944	23.149	23.513	25.697	7.321	11.007	9.288
<b>0.8</b>	22.365	21.03	21.539	25.006	11.809	18.906	16.096
<b>0.9</b>	20.851	19.194	19.838	24.332	<b>16.695</b>	<b>26.769</b>	<b>22.653</b>

*Reducing Random-Valued Impulse Noise in Digital Color Images*

Table 6. The RMSE of the VMF, ARWSF and AST methods to the IMF-KM method.

<b>P</b>	VMF	ARWSF	AST	IMF-KM	VMF (%↑)	ARWSF (% ↑)	AST (%↑)
<b>0.1</b>	0.1374	0.1405	0.1414	0.1413	2.838	0.569	2.838
<b>0.2</b>	0.1364	0.14	0.141	0.1408	3.226	0.571	3.226
<b>0.3</b>	0.1354	0.1397	0.1406	0.1404	3.693	0.501	3.693
<b>0.4</b>	0.1337	0.1389	0.1396	0.1398	4.562	0.648	4.562
<b>0.5</b>	0.1319	0.1381	0.1388	0.1393	5.610	0.869	5.610
<b>0.6</b>	0.1288	0.1358	0.1366	0.1387	7.686	2.135	7.686
<b>0.7</b>	0.1252	0.1332	0.1338	0.138	10.224	3.604	10.224
<b>0.8</b>	0.1208	0.1285	0.1297	0.1371	13.493	6.693	13.493
<b>0.95</b>	0.1116	0.1166	0.1194	0.1348	<b>20.789</b>	<b>15.609</b>	<b>20.789</b>

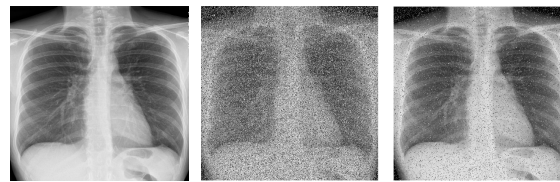
diagnosis for radiologists as it is more time-saving and aids in rapid screening of suspected cases [20, 21]. For a long time, image processing has been used to assist radiologists in more accurate diagnosis by filtering out the noise due to thermal spikes or electrical effects in X-ray or CT-scan images. In the context of the COVID-19 outbreak, this has become much more critical for improved and faster diagnosis. In the context of the COVID-19 outbreak, this has become much more critical for improved and faster diagnosis. Image processing and machine learning methods have been successfully used for improved COVID-19 diagnosis from CT scans [22].

Here we implement the proposed IMF-KM method on CT scan images on patients diagnosed with COVID-19 (courtesy: <https://github.com/agchung/COVID-chestxray/dataset/tree/master/images>). The CT scans are grayscale images and hence we do not have the three-color components but the methodology of our proposal remains unchanged. We implemented five test cases infected with COVID-19 and one test case with no infection. All the CT scans are embedded with the impulse noise described in Eq. (3) with noise probability  $p = 0.5$ . Figure 13 shows the results. It can be observed that the noisy images contain so much impulsive noise so it would adversely affect the diagnosis and the consequent prognosis of the patient. It can be observed in the last column of each row (the filtered output images) that the proposed IMF-KM method denoises the CT scans to the extent of being very close to the originally obtained scan.

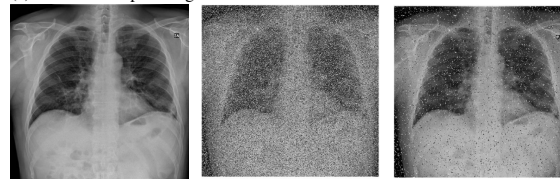
To showcase the superiority of the noise reduction methods, it is a common practice to artificially add noise and then demonstrate the strength of the conventional filters in reducing it. The same has been performed in this paper to this point. Taking a different approach, we now consider the CT scan of a COVID-19-infected patient in its original form and then perform filtering on it treating it to have been minutely affected by impulse noise. This is shown in Fig. 14. Medical research has deduced that the CT scans of a COVID-19-infected patient tend to have white patches which signify the combination of pus and water indicating respiratory complications.

The key strength of the proposed IMF-KM method is to especially filter out the noise contamination at the edges by virtue of considering the most identical pixels. This feature straightforwardly helps in averaging out the noise at the edges of the

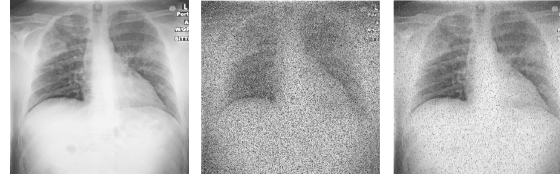
*S. R. Gantepalli & P. B. Choppala*



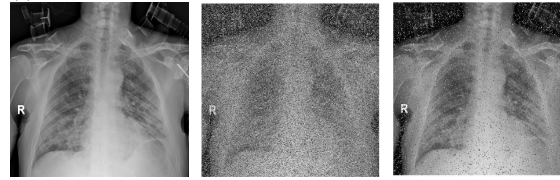
(i) Test case 1 (COVID-19 positive): left to right (a) original, (b) noisy and  
(c) IMF-KM output images



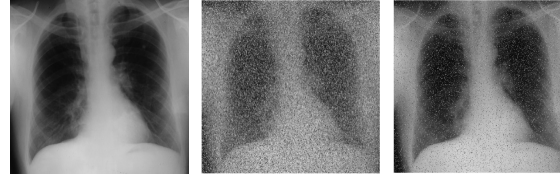
(ii) Test case 2 (COVID-19 positive): left to right (a) original, (b) noisy and  
(c) IMF-KM output images



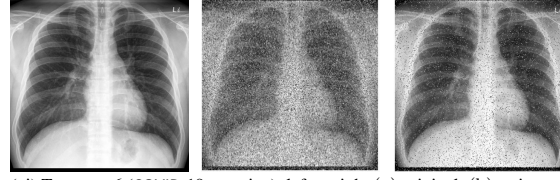
(iii) Test case 3 (COVID-19 positive): left to right (a) original, (b) noisy and  
(c) IMF-KM output images



(iv) Test case 4 (COVID-19 positive): left to right (a) original, (b) noisy and  
(c) IMF-KM output images



(v) Test case 5 (COVID-19 positive): left to right (a) original, (b) noisy and  
(c) IMF-KM output images



(vi) Test case 6 (COVID-19 negative): left to right (a) original, (b) noisy and  
(c) IMF-KM output images

Fig. 13. This figure shows the six test cases of CT scans with the original image along the left column, the noisy image in the middle, and the IMF-KMS filtered output in the last, with noise probability  $p = 0.5$ .

## Reducing Random-Valued Impulse Noise in Digital Color Images

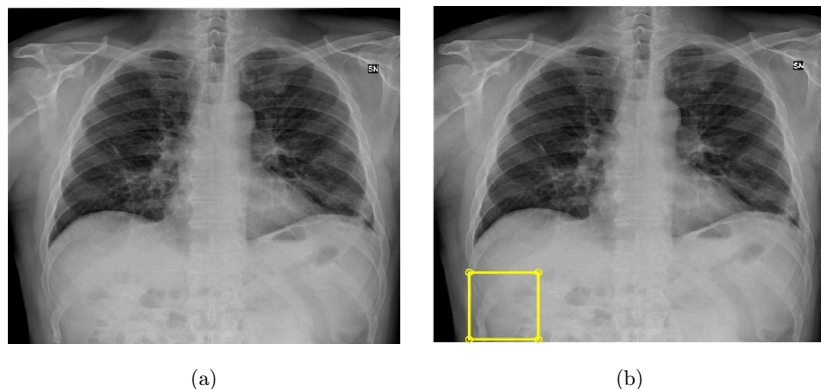


Fig. 14. Test case (COVID-19 positive): left to right (a) original and (b) IMF-KM output images.

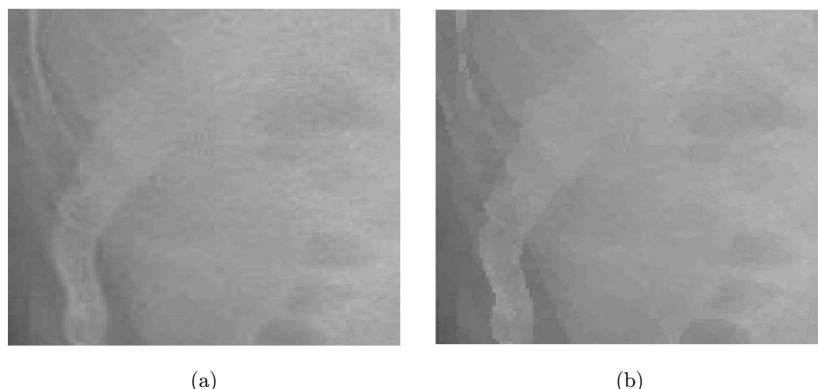


Fig. 15. Left to right (a) original and (b) IMF-KM filtered output images, of the yellow patch shown in Fig. 14. It can be seen that the filtered output differentiates the colors more accurately than the original laboratory image.

bone and allows the signal to protrude from the noise. A patch of Fig. 14 (shown in a yellow rectangle) is shown to demonstrate this effect in Fig. 15. Here it can be observed that the white and dark patches are well-differentiated and aid in improved diagnosis for a radiologist. This property is helpful in COVID-19 cases in which the CT scan has white patches near the lower part of the lungs signifying partial filling of air space, termed ground-glass opacity [23].

### 5.2. Application to visual tracking

Visual tracking is an important field of engineering and used for object detection and tracking in robotics, radar and sonar applications. The visual tracking algorithms employ a time recursion filtering process to predict and update moving target(s) using noisy image measurements [24]. These noisy image measurements should first

S. R. Gantepalli & P. B. Choppala



Fig. 16. This figure shows 25 snapshots in rows of a single target (ant) moving on a paper. In each row, the left figure corresponds to the original image, the middle to the noisy image and the right to the filtered output image.

*Reducing Random-Valued Impulse Noise in Digital Color Images*Fig. 16. (*Continued*)

*S. R. Gantepalli & P. B. Choppala*

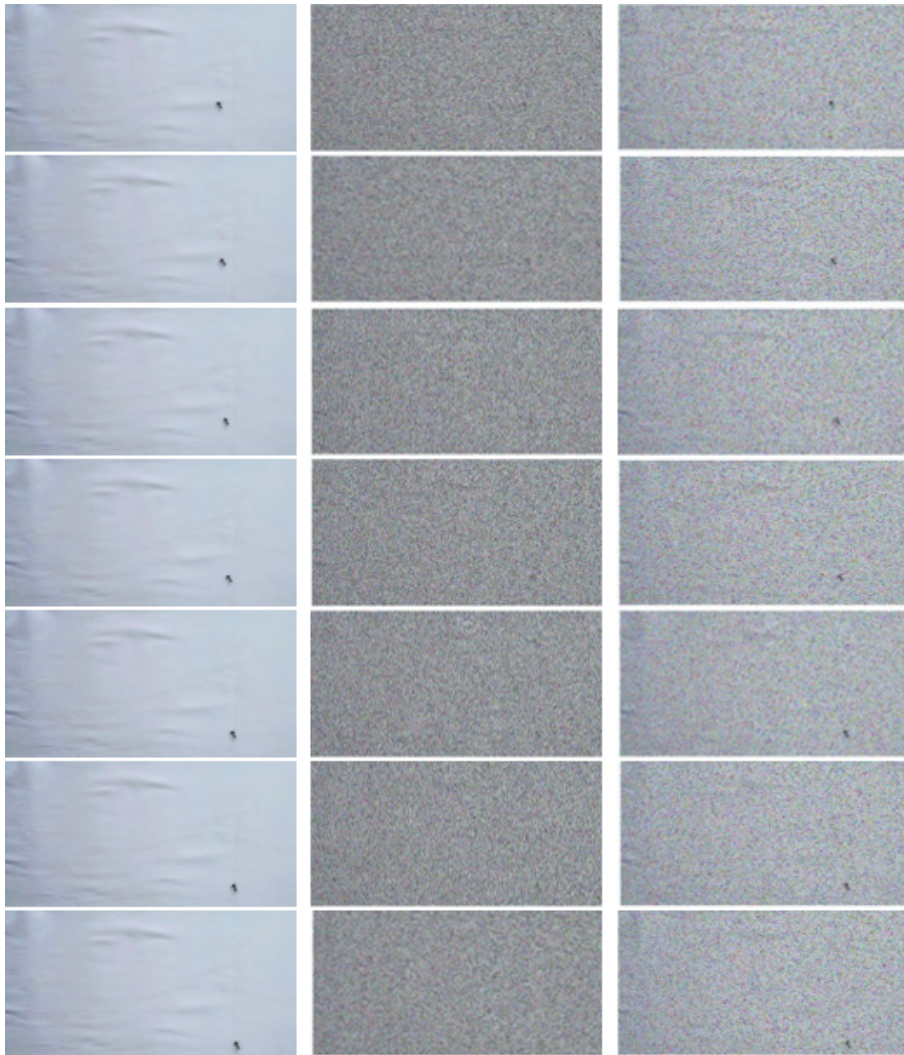


Fig. 16. (*Continued*)

be preprocessed for improved tracking performance and this is where image noise reduction schemes become critical. In this section, we demonstrate the efficacy of the proposed IMF-KM method in extracting the hidden target from noisy images. This demonstration for a period of 25-time steps is shown in Fig. 16. It can be observed that it is nearly impossible to detect the target (ant) from the noisy images (the middle column). It is also nearly impossible to detect the target by observing a sequence of frames. Any visual tracker is set to fail for such high noise scenarios. Whereas it can be seen that the proposed IMF-KM method (the last column)

*Reducing Random-Valued Impulse Noise in Digital Color Images*

extracts the target from the noise with very high accuracy. It is both possible to detect the target from one frame and also from a sequence of frames. This performance is by virtue of filtering the most informative pixels in a chosen window by means of  $k$ -means clustering.

The tracking algorithms employ a time recursion filtering process to predict and update the moving target(s) using noisy image measurements [24, 25].

The proposed clustering method has several limitations. One significant limitation is its dependency on the initial choice of values or features, which may not always capture the most relevant aspects of the image for clustering. Additionally, the method can be sensitive to noise and outliers in the data, potentially leading to incorrect or unstable cluster formations. The performance of the clustering algorithm can also be affected by the choice of parameters, such as the number of clusters in  $k$ -means, which may not be straightforward to determine optimally. Furthermore, the method may struggle with images that have complex or overlapping patterns, resulting in ambiguous cluster boundaries. It can also be computationally intensive, especially for large images or datasets, making it less practical for real-time applications. Lastly, the method may require significant preprocessing and post-processing steps to achieve accurate and meaningful segmentation, adding to the overall complexity. Despite its limitations, the proposed clustering method proves to be more effective at higher noise levels compared to low noise levels. This effectiveness arises because the clustering algorithm can average out noise over larger regions, making the clusters more robust against random fluctuations. In high-noise environments, the method's ability to distinguish significant patterns and features becomes more pronounced, allowing it to segment the image more accurately. The inherent redundancy in noisy data helps the algorithm to identify and group similar pixels, enhancing the overall clustering performance. Consequently, the method's robustness in high noise conditions highlights its potential for applications where noise is a prevalent issue.

### **5.3. Evaluation of dataset**

The thorough evaluation of the proposed method on a dataset of 72 images has yielded important insights into its effectiveness. Both the proposed method and the state-of-the-art techniques used for comparison in the paper were tested on this dataset (accessible at <https://bit.ly/3w3Qstf>), and the resulting filtered images can be viewed at <https://rb.gy/3t190k>.

## **6. Conclusion**

This paper proposed isolated vector median filtering with  $k$ -means clustering for noise reduction in digital color images. The method is two-fold, one to categorize the pixels in the sliding window into two groups, one that contributes to the signal and the other that contributes to the noise, and then to perform median filtering, in isolation of the color components, over the pixel intensities that contribute to the

*S. R. Gantengapalli & P. B. Choppala*

signal. The key merit of this proposal is that using only the useful pixels for median filtering in isolation of the color components will result in smoothing that stays local and does not affect the other color components and hence leads to improved accuracy in image reconstruction. We have demonstrated the superiority of the proposed method using real images and several statistical measures. We also implemented the proposed method on COVID-19 CT scan images and discussed its efficacy in aiding the radiologist in the improved medical diagnosis of these scans. The method is also implemented successfully as a preprocessing tool for a visual tracking example. In the future, we will incorporate clustering methods within more sophisticated noise reduction schemes for targeted diagnosis of COVID-19 CT scan images.

### Acknowledgment

The method of isolated vector median filtering using  $k$ -means clustering presented in this paper has been patented under Application No. 202241004435 A on 04/02/2022 with the title ‘A system for noise reduction in digital color images’.

### ORCID

Srinivasa Rao Gantengapalli  <https://orcid.org/0000-0001-8034-3430>

Praveen Babu Choppala  <https://orcid.org/0000-0002-7360-1822>

### References

- [1] D. N. H. Thanh, N. V. Son and V. B. S. Prasath, An adaptive method for image restoration based on high-order total variation and inverse gradient, *Signal Image Video Process.* **14** (2020) 1181–1190.
- [2] H. Parsiani, Isolated noise detection and reduction in color images, *IEEE Proc. 36th Midwest Symposium on Circuits and Systems* (Detroit, MI, USA, 1993), pp. 741–743.
- [3] A. K. Yadav, R. Roi, R. K. C. Sandesh Kumar and A. P. Kumar, Algorithm for de-noising of color images based on median filter, *IEEE Conf. Image Information Processing* (Waknaghat, India, 2015).
- [4] R. Lukac, B. Smolka, K. Martin, K. N. Plataniotis and A. N. Venetsanopoulos, Vector filtering for color imaging, *IEEE Signal Process. Magaz.* **74** (2005) 74–86.
- [5] X. Yang and T. Zhang, Color image denoising using adaptive filtering and color space transformations, *IEEE Trans. Image Process.* **30**(4) (2021) 1001–1012.
- [6] J. Astola, P. Haavisto and Y. Neuvo, Vector median filters, *Proc. IEEE* **78**(4) (1990) 678–689.
- [7] A. S. Kumar and R. C. Prasad, An efficient color image filtering algorithm for impulse noise removal, *Signal Process. Image Commun.* **75** (2019) 18–27.
- [8] Y. S. Wang and Y. L. Huang, Edge-preserving impulse noise removal for color images, *J. Visual Commun. Image Represent.* **38** (2016) 492–502.
- [9] P. E. Trahanias and A. N. Venetsanopoulos, Vector directional filters-a new class of multichannel image processing filters, *IEEE Trans. Image Process.* **2**(4) (1993) 528–534.

## Reducing Random-Valued Impulse Noise in Digital Color Images

- [10] D. G. Karakos and P. E. Trahanias, Combining vector median and vector directional filters: The directional distance filters, *IEEE Proc. Int. Conf. Image Process.*, Vol. 1 (1995), pp. 171–174.
- [11] S. Vinayagamoorthy, K. N. Plataniotis, D. Androutsos and A. N. Venetsanopoulos, A multichannel filter for TV signal processing, *IEEE Trans. Consum. Electron.* **42**(2) (1996) 199–205.
- [12] G. George, R. M. Oommen, S. Shelly, S. S. Philipose and A. M. Varghese, A survey on various median filtering techniques for removal of impulse noise from digital image, *IEEE Conf. Emerg. Dev. Smart Syst.* (2018) 235–238.
- [13] R. Chanu and K. M. Singh, Vector median filters: A survey, *Int. J. Comput. Sci. Netw. Secur.* **16**(12) (2016) 66–84.
- [14] B. Smolka, K. Malik and D. Malik, Adaptive rank weighted switching filter for impulsive noise removal in color images, *J. Real-Time Image Process.* **10**(2) (2015) 289–311.
- [15] C. Kenney, Y. Deng, B. S. Manjunath and G. Hewer, Peer group image enhancement, *IEEE Trans. Image Process.* **10**(2) (2001) 326–334.
- [16] X. Zhang and X. Youlun, Impulse noise removal using directional difference-based noise detector and adaptive weighted mean filter, *IEEE Signal Process. Lett.* **16**(4) (2009) 295–298.
- [17] R. Lukac, B. Smolka, K. Martin, K. N. Plataniotis and A. N. Venetsanopoulos, Vector filtering for color imaging, *IEEE Signal Process. Magaz.* **22**(1) (2005) 74–86.
- [18] J. MacQueen, Some methods for classification and analysis of multivariate observations, *Proc. Fifth Berkeley Symp. Math. Stat. Prob.* **1**(15) (1967) 281–297.
- [19] P. B. Choppala, J. S. Meka and P. V. G. D. Prasad Reddy, Vector isolated minimum distance filtering for image de-noising in digital color images, *Int. J. Recent Technol. Eng.* **8**(4) (2020) 2402–2405.
- [20] P. B. Choppala, J. S. Meka and P. V. G. D. Prasad Reddy, Isolated vector median filtering for noise reduction in digital color images, *Int. J. Adv. Sci. Technol.* **29**(6) (2020) 8305–8317.
- [21] T. Kanungo, D. M. Mount, N. S. Netanyahu, C. D. Piatko, R. Silverman and A. Y. Wu, An efficient k-means clustering algorithm: Analysis and implementation, *IEEE Trans. Pattern Anal. Mach. Intel.* **24**(7) (2002) 881–892.
- [22] E. D. Tenda, M. Yulianti, M. M. Asaf, R. E. Yunus, W. Septiyanti, V. Wulani, C. W. Pitoyo, C. M. Rumende and S. Setiati, The importance of chest CT scan in COVID-19: A case series, *Acta Med Indonesiana — Indones. J. Internal Med.* **52**(1) (2020) 68–73.
- [23] I. Abdollahi, M. Nabahati, M. Javanian, H. Shirafkan and R. Mehraeen, Can initial chest CT scan predict status and clinical outcomes of COVID-19 infection? A retrospective cohort study, *Egypt. J. Radiol. Nuclear Med.* **158** (2021) 1–10.
- [24] W. Zhao, W. Jiang and X. Qiu, Deep learning for COVID-19 detection based on CT images, *Sci. Rep.* **11** (2021) 14353.
- [25] S. Sharma, Drawing insights from COVID-19-infected patients using CT scan images and machine learning techniques: A study on 200 patients, *Environ. Sci. Pollut. Res.* **27** (2020) 37155–37163.
- [26] J. Vermaak, S. Maskell, M. Briers and P. Perez, Bayesian visual tracking with existence process, *IEEE Int. Conf. Image Process.* Vol. 1 (2005), pp. 721–724.
- [27] N. Oliver, B. Rosario and A. Pentla, A Bayesian computer vision system for modeling human interactions, *IEEE Trans. Pattern Anal. Mach. Intel.* **22**(8) (2000) 1–18.